# Small Metal-Containing Oligomers Using $M_2(dmpm)_x$ and $M_2(dmb)_y$ Luminescent Building Blocks (M = Cu, Ag; $x$ = 2, 3; $y$ = 1, 2)

Éric Fournier,[a] Andreas Decken,[b] and Pierre D. Harvey*[a]

**Keywords:** Coordination polymers / Oligomers / Silver / Copper / Luminescence

The luminescent binuclear complexes $M_2(dmpm)_3^{2+}$ [M = Cu, Ag; dmpm = bis(dimethylphosphanyl)methane], $Ag_2(dmpm)_2^{2+}$ and $Cu_2(dmpm)_3(CN\text{-}tBu)_2^{2+}$ (as $BF_4^-$ salts), as well as the oligomers described as $\{Cu_2(dmpm)_3(dmb)_{1.33}^{2+}\}_3$ and $\{Ag_2(dmpm)_2(dmb)_{1.33}^{2+}\}_3$ (dmb = 1,8-diisocyano-*p*-menthane), have been prepared and fully characterized in the solid state. These compounds exhibit emission maxima ranging from 445 to 485 nm with emission lifetimes in the μs time scale. The X-ray structures for the $M_2(dmpm)_3^{2+}$ (M = Cu, Ag) and $Cu_2(dmpm)_3(CN\text{-}tBu)_2^{2+}$ complexes, XRD patterns (X-ray powder diffraction), DSC (differential scanning calorimetry), TGA (thermal gravimetric analysis), and the solid-state IR spectra have been examined in order to characterize these complexes and oligomers.


## Introduction

The synthesis and characterization of transition-metal-containing coordination and organometallic oligomers and polymers built with phosphane and isocyanide assembling ligands is becoming a topic of increasing interest in the quest for new materials and applications.[1−14] In this respect, our group has recently reported the syntheses and characterizations of 1-D polymers of the type $\{M(dmb)_2^+\}_n$ [15,16] and the mixed-ligand polymers $\{M_2(dppm)_2(dmb)_2^{2+}\}_n$ [17] (M = Cu, Ag; dmb = 1,8-diisocyano-*p*-menthane in its *U*- or *Z*-conformation; dppm = bis(diphenylphosphanyl)-methane; Scheme 1). The chromophores are the $M(C{\equiv}NR)_4^+$ centers (M = Cu, Ag), which are separated by 5 Å (Ag···Ag distance) in $\{Ag(dmb)_2^+\}_n$,[15] and the $M(C{\equiv}NR)_2(P)_2^+$ units, which are separated by 4.03 and 9.61 Å in $\{Ag_2(dppm)_2(dmb)_2^{2+}\}_n$.[17]

The average polymer length for the $\{Ag(dmb)_2^+\}_n$ materials in solution was determined to be approximately 8 units by $T_1$/NOE measurements,[18] whereas the amorphous Cu analogue had an average polymer length of 300 units, as determined by light scattering.[15] This difference is explained by the greater lability of the dmb ligand in the $Ag^I$ complexes, which was convincingly verified by the interconversion observed between the *U*- and *Z*-isomers of the $\{Ag(dmb)_2^+\}_n$ polymers, but not for the Cu analogues.[19] Ligand dissociation has also been established in previous works on the $\{Pd_4(dmb)_4(dmb)^{2+}\}_n$ [6] and $\{Pt_4(dmb)_4(diphos)^{2+}\}_n$ [7] polymers [diphos = $Ph_2P(CH_2)_mPPh_2$; $m$ = 4−6; 84000 < $MW_n$ < 307000; Scheme 2]. There are also some differences in the photophysical data, in particular the emission lifetimes, between the polymers and the corresponding building blocks [here $M_4(dmb)_4^{2+}$ (M = Pd, Pt)].

More recently, a new series of amorphous polymeric materials of the type $\{M(diphos)(dmb)^+\}_n$ (M = Cu, Ag),[22] $\{Pd_2(diphos)_2(dmb)^{2+}\}_n$ (diphos = dppe, dppp),[22] $\{Pd_2(dmb)_2Cl_2\}_n$,[23] and $\{Pd_2(dmb)_2(diphos')^{2+}\}_n$ (diphos′ = dppb, dpppen, dpph)[23] (Scheme 3) were prepared and characterized. It was clearly demonstrated that polymers in the solid state dissociated to give oligomers in solution (8−16 units).

We now wish to report the syntheses and characterizations of new $Cu^I$ and $Ag^I$ binuclear and oligomeric complexes using the bridging diisocyanide dmb and electron-rich diphosphane dmpm ligands. By changing the nature of the assembling ligands and building blocks, one can hope not only to change the distance between the building blocks, but also to change the number of units. These oligomers are composed of the following building blocks: $M_2(dmpm)_3^{2+}$,[24−26] $Ag_2(dmpm)_2^{2+}$,[24−26] $M_2(dmb)_2^{2+}$ (M = Ag, Cu),[27−29] and $Ag_2(dmb)^{2+}$ [15−16] (Scheme 4).

## Results and Discussion

### The $M_2(dmpm)_x^{2+}$ Building Blocks

The binuclear $M_2(dmpm)_3^{2+}$ complexes [M = Cu (**1**), Ag (**2**)] are synthesized by the direct reaction between dmpm and the desired metal cationic species in the appropriate stoichiometric ratio. In a 1:1 stoichiometric ratio, the dmpm ligand also reacts with $AgBF_4$ to form the dicoordinated

[a] Département de Chimie, Université de Sherbrooke, Sherbrooke J1K 2R1, PQ., Canada
Fax: (internat.) + 1 819-821-8017
E-mail: p.harvey@Usherbrooke.ca
[b] Department of Chemistry, University of New Brunswick, Fredericton E3B 6E2, New Brunswick, Canada
E-mail: adecken@unb.ca

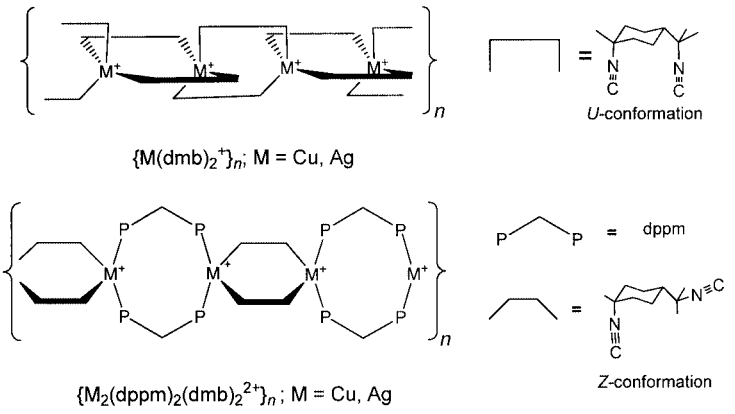


Scheme 1

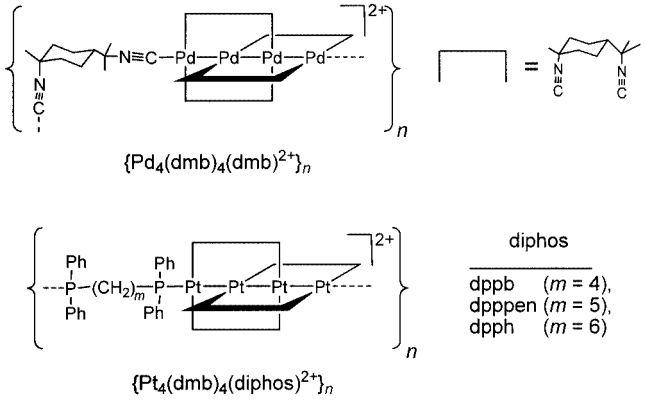


Scheme 2

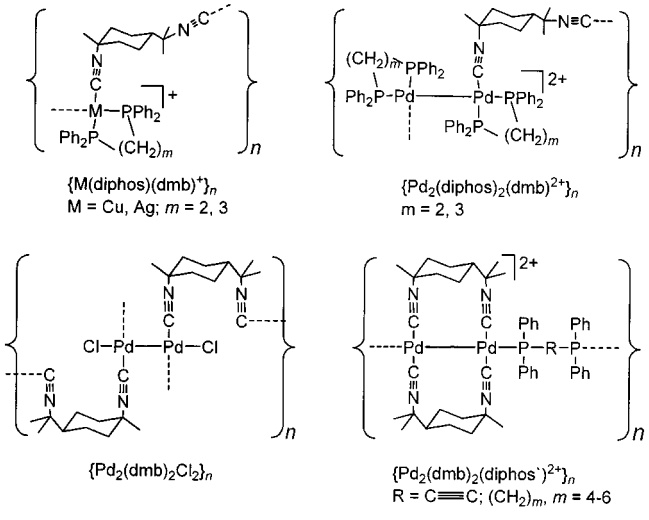


Scheme 3

dimer $Ag_2(dmpm)_2^{2+}$ (**3**). Complexes **2** and **3** can be distinguished by their sensitivity to light (**3** turns gray with time) and by $^{31}P$ NMR spectroscopy.

Crystals suitable for X-ray single-crystal analysis were obtained for **1** and **2**. (Figures 1 and 2, Table 1 and Table 7). The complexes exhibit two nearly trigonal planar coordinated metal atoms positioned face-to-face, and separated by 2.9265(3) and 2.9893(2) Å, for **1** and **2**, respectively. The separation in **1** is significantly shorter than that in the $[Cu_2(dmpm)_3](ClO_4)_2$ salt [3.021(2)Å],[26] and the distances for **1** and **2** fall short in comparison with the isostructural $Au_2(dmpm)_3^{2+}$ analogue (3.040 and 3.050 Å).[30] The average M···M distances follow the trend of their respective ionic radii ($Cu^I$, 0.91 Å < $Ag^I$, 1.29 Å < Au, 1.51 Å).[31] The $Ag_2$ and $Au_2$ distances are shorter than the sum of the van der Waals radii (3.4 Å)[31] indicating the presence of $M_2$ interactions, but this is not the case for the $Cu_2$ distance in **1** (2.8 Å).[31] The average PCuCu angle is not 90°, but slightly bent inward (88.3°), which may suggest the presence of weak $M_2$ interactions in this case. In addition, the AgP distances (average 2.434 Å) are longer than the CuP and AuP distances (Table 2), and do not follow the change in ionic radii. This is perfectly consistent with the findings of Schmidbaur et al., which state that Ag is larger than Au due to relativistic effects[32] but the M···M data presented above do not support this argument. The aurophilicity may be more important than the argentophilicity in this case.

The neutral isoelectronic $M_2(dppm)_3$ dimers (M = Pd,[33] Pt[34]) exhibit $M_2$ distances similar to their neighboring atoms in the periodic table (Pd ~ $Ag^+$; Pt ~ $Au^+$), but the cationic systems show slightly longer $M_2$ distances (Table 2), most likely reflecting internuclear electrostatic repulsion. Remarkably, the $d(Ag_2)$ value for $[Ag_2(dmpm)_2](PF_6)_2$ [3.041(1)Å][35] is longer than that found in **2**, indicating that the third dmpm ligand applies some extra restoring force. This is further exemplified in the $Cu_2(dmpm)_2(O_2CMe)^+$ complex, in which the shorter bite distance of the acetate ligand forces the Cu atoms to lie closer to one another [2.7883(11)Å][36] in comparison with **1**.

The model compound **4** was prepared by the direct reaction between **1** and 2 equivalents of *t*BuNC. Despite the poor quality of the single crystals [$a$ = 24.935(4), $b$ = 10.5070(15), $c$ = 19.266(3) Å, β = 111.034(2)°, $V$ =

  

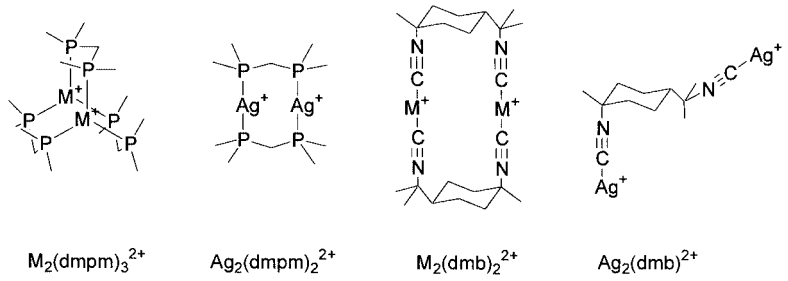


Scheme 4

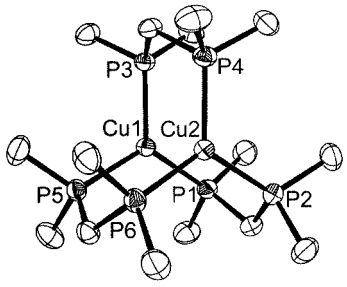


Figure 1. Thermal ellipsoid plots for **1**; the ellipsoids are shown with 30% probability; the H atoms and $BF_4^-$ ions are not shown for clarity

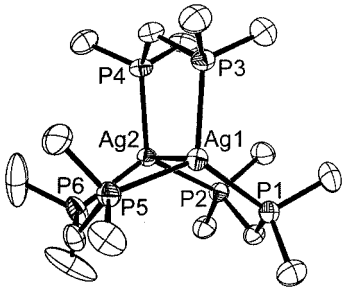


Figure 2. Thermal ellipsoid plots for **2**; the ellipsoids are shown with 30% probability; the H atoms and $BF_4^-$ ions are not shown for clarity

Table 1. Selected bond lengths [Å] and angles [°] for **1** (left) and **2** (right)

| | | | |
|---|---|---|---|
| Cu(1)−Cu(2) | 2.9265(3) | Ag(1)−Ag(2) | 2.9893(2) |
| Cu(1)−P(1) | 2.2484(5) | Ag(1)−P(1) | 2.4415(5) |
| Cu(1)−P(3) | 2.2519(5) | Ag(1)−P(3) | 2.4537(5) |
| Cu(1)−P(5) | 2.2463(5) | Ag(1)−P(5) | 2.4774(5) |
| Cu(2)−P(2) | 2.2329(5) | Ag(2)−P(2) | 2.4403(5) |
| Cu(2)−P(4) | 2.2392(5) | Ag(2)−P(4) | 2.4246(5) |
| Cu(2)−P(6) | 2.2378(5) | Ag(2)−P(6) | 2.4378(5) |
| P(5)−Cu(1)−P(1) | 120.12(2) | P(1)−Ag(1)−P(5) | 120.298(18) |
| P(5)−Cu(1)−P(3) | 118.11(2) | P(3)−Ag(1)−P(5) | 113.530(18) |
| P(1)−Cu(1)−P(3) | 121.67(2) | P(1) −Ag(1)−P(3) | 126.122(18) |
| P(2)−Cu(2)−P(6) | 118.74(2) | P(2)−Ag(2)−P(6) | 117.882(18) |
| P(2)−Cu(2)−P(4) | 121.19(2) | P(4)−Ag(2)−P(2) | 119.69(2) |
| P(6)−Cu(2)−P(4) | 119.53(2) | P(4)−Ag(2)−P(6) | 122.16(2) |
| P(5)−Cu(1)−Cu(2) | 92.475(15) | P(5)−Ag(1)−Ag(2) | 89.931(13) |
| P(1)−Cu(1)−Cu(2) | 89.760(16) | P(1)−Ag(1)−Ag(2) | 92.317(13) |
| P(3)−Cu(1)−Cu(2) | 90.888(15) | P(3)−Ag(1)−Ag(2) | 85.399(14) |
| P(2)−Cu(2)−Cu(1) | 93.963(16) | P(2)−Ag(1)−Ag(2) | 88.852(13) |
| P(6)−Cu(2)−Cu(1) | 90.983(15) | P(6)−Ag(1)−Ag(2) | 91.912(13) |
| P(4)−Cu(2)−Cu(1) | 92.386(15) | P(4)−Ag(1)−Ag(2) | 94.312(14) |

4711.2(12) Å$^3$, $Z = 8$, $d = 2.061$ Mg/m$^3$, $R_1 = 0.22$; $wR_2 = 0.55$] both the spectra and crystallographic data are consistent with the addition of 2 *t*BuNC ligands at the axial positions of the $Cu_2(dmpm)_3^{2+}$ skeleton (Scheme 5).

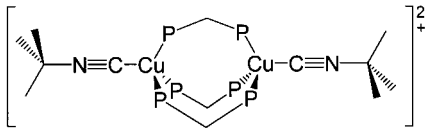


$Cu_2(dmpm)_3(CN\text{-}tBu)_2^{2+}$

Scheme 5

The Cu···Cu separation is found to be 4.011 Å, where no Cu···Cu interaction is noted. The structure exhibits similarities with the $d^{10}$-$d^{10}$ complex $Pt_2(dppm)_3(PPh_3)$,[37] in which one Pt atom adopts a tetracoordinate geometry causing an increase in the Pt···Pt distance with respect to $Pt_2(dppm)_3$.[33,34]

Table 2. Comparison of selected structural data for $d^{10}$-$d^{10}$ $M_2(dmpm)_3^{2+}$ and $M'_2(dppm)_3$ dimers

| | $d(M_2)$ [Å] | $2r_{vdw}$ [Å] | $d$[(MP)$_{av}$] [Å] | Approx. point group | Refs. |
|---|---|---|---|---|---|
| $Cu_2(dmpm)_3^{2+}$ ($BF_4^-$) | 2.9265(3) | 2.80 | 2.243(10) | $C_s$ | this work |
| $Cu_2(dmpm)_3^{2+}$ ($ClO_4^-$) | 3.021(2) | 2.80 | 2.245(6) | $C_s$ | [26] |
| $Ag_2(dmpm)_3^{2+}$ | 2.9893(2) | 3.40 | 2.434(31) | $C_s$ | this work |
| $Au_2(dmpm)_3^{2+}$ | 3.040(1) 3.050(1) | 3.40 | 2.358 | $C_s$ | [40] |
| $Pd_2(dppm)_3$ | 2.956(1) | 3.20 | 2.310(10) | $C_3$ | [42] |
| $Pt_2(dppm)_3$ | 3.022(3) | 3.50 | 2.265(3) | $C_3$ | [43][44] |

  

No attempt was made to synthesize the $\{Ag_2(dmpm)_2(CN\text{-}tBu)_2\}^{2+}$ complex, as the crystallographically characterized $[Ag_2(dppm)_2(CN\text{-}tBu)_2](ClO_4)_2$ complex was recently reported by us (Scheme 6).[17] The structure consists of two face-to-face tricoordinate $Ag^I$ atoms bridged by two dppm ligands, where one CN-*t*Bu ligand binds each of the metals, similar to that in $Ag_2(dmpm)_3^{2+}$ with the difference that one diphosphane ligand is replaced by two isocyanide groups.

### Synthesis and Characterization of the Oligomers

Compound **1** and dmb reaction ratios varying from 1:1 to 1:2, invariably forming an oligomeric material best described as $[Cu_6(dmpm)_9(dmb)_4](BF_4)_6$ or $\{[Cu_2(dmpm)_3(dmb)_{1.33}](BF_4)_2\}_2$ (**5**). This formulation, $[Cu_2(dmpm)_3(dmb)^{2+}]_x(dmb)$ ($x = 3$), is unambiguously established from the reproducible chemical analyses, integration of the $^1H$ NMR data (dmpm vs. dmb), and TGA data (Table 3). It is possible that traces of shorter and longer oligomers ($x = 1$, 2 and $x > 3$) exist, but the product distribution must be very narrow since the oligomer is very small, and all three techniques above indicate the same results. If such oligomers exist, their concentration must be very low. The XRD spectra indicate the presence of a highly crystalline material, which is consistent with the oligomeric nature of the material, but also support the hypothesis for a very narrow product distribution. The chemical yield is modest, indicating some losses during the attempts to obtain pure samples. The short oligomeric nature of the material is also confirmed by the observed ν(N≡C) absorption for uncoordinated isocyanides at 2132 $cm^{-1}$ in the solid-state IR spectra (Figure 3), indicating that its relative presence is important in comparison with the coordinated ones (2161 $cm^{-1}$). Long chains ending with dmb ligands would exhibit very weak absorption due to uncoordinated isocyanides relative to the coordinated ones.

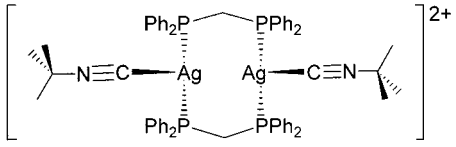


Scheme 6

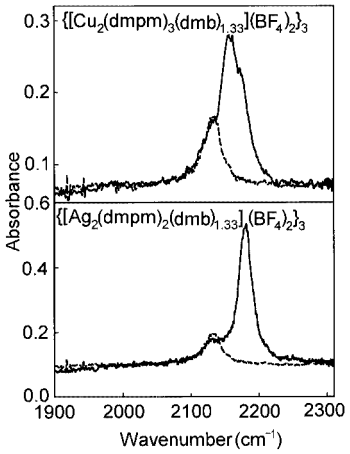


Figure 3. Solid state FT-IR spectra of **5** (top) and **6** (bottom) in the ν(N≡C) region (−) in comparison with free dmb (- - - -), emphasizing evidence of non-coordinated −N≡C groups in the oligomers

The corresponding $Ag_2(dmpm)_3^{2+}$ complex does not react with dmb even in excess. This behavior may reflect the fact that dmpm is a strong σ-donor, which renders the $Ag^I$ atoms significantly more electron-rich. As a result, the monodentate RNC ligands become very labile. Conversely, the $Ag_2(dmpm)_2^{2+}$ complex reacts with dmb in a 1:1 ratio to generate another oligomeric material, identified as $[Ag_6(dmpm)_6(dmb)_4](BF_4)_6$ or $\{[Ag_2(dmpm)_2(dmb)_{1.33}](BF_4)_2\}_3$ (**6**) by reproducible chemical analysis, $^1H$ NMR spectroscopy and TGA. Oligomer **6** is also a crystalline solid (XRD). The MALDI-TOF spectra for both **5** and **6** are very complex, where fragment peaks show evidence for M−P, P−C, and C−N bond cleavage. In both cases, the molecular ion was not observed. Size-exclusion chromatography was also inadequate, as the compounds tended to stay trapped in the column, despite the use of different column materials. Both oligomeric materials crystallize to form long needle-shaped crystals, a shape that is common for dmb-containing polymers, but the thickness of these needles was inadequate for X-ray analysis. IR characteristics similar to those described for **5** above are depicted in the spectra of **6**, where a weak absorption associated to free ν(N≡C) is observed (Figure 3). It is interesting to note that both oligomers **5** and **6** (6 metal atoms) exhibit a lower degree of oligomerization than that reported for $\{[Ag(dmb)_2]BF_4\}_n$ in solution ($n = 7-8$).[18]

Table 3. TGA data for **1**, **4**, **5**, and **6**

| Compounds | | Weight loss 1[a] | | | Weight loss 2[a] | | | Residue | |
|---|---|---|---|---|---|---|---|---|---|
| | | Temp. Range (°C) | Exp. % | Theor. % | Temp. Range (°C) | Exp. % | Theor. % | Exp. % | Theor. % |
| 1 | $[Cu_2(dmpm)_3](BF_4)_2$ | − | − | − | 320−390 | 86 | 81 | 14 | 19 |
| 4 | $[Cu_2(dmpm)_3(CN\text{-}tBu)_2](BF_4)_2$ | 120−190 | 19 | 19 | 320−390 | 66 | 66 | 15 | 15 |
| 5 | $\{[Cu_2(dmpm)_3(dmb)_{1.33}](BF_4)_2\}_3$ | 210−230 | 27 | 26 | 300−390 | 60 | 61 | 13 | 13 |
| 6 | $\{[Ag_2(dmpm)_2(dmb)_{1.33}](BF_4)_2\}_3$ | 180−210 | 28 | 29 | 290−345 | 46 | 48 | 26 | 23 |

[a] Weight loss 1 is due to the loss of *t*BuNC or dmb; weight loss 2 is due to the loss of dmpm and $BF_4$; the uncertainties are ±2% based on the small drift of the baseline.

  

No glass transition (or other thermal phenomenon) was observed between −20 °C and 100 °C in the DSC traces for any of the investigated compounds. The result is consistent with the nonpolymeric nature of the materials.

### Modeling

In the absence of X-ray data, the model compounds $Ag_2(dmpm)_2(CN\text{-}tBu)_2^{2+}$ and $Cu_4(dmpm)_6(dmb)_2(CN\text{-}tBu)^{4+}$ were computed to address two specific questions. Is the Ag···Ag distance in $Ag_2(dmpm)_2(CN\text{-}tBu)_2^{2+}$ (model compound for **6**) similar to $Ag_2(dmpm)_3^{2+}$ (explaining some similarities in the electronic spectra), and what distance separates the different dimer units in **5** (and ultimately in **6** as well)?

The methodology has been tested on the X-ray data for **1**, **2**, and the related binuclear complex $[Ag_2(dppm)_2(CN\text{-}tBu)_2](ClO_4)_2$[17] (Table 4) in order to provide a degree of confidence in the results. The M···M and M···P distances are computed within an uncertainty of 0.05−0.06 Å, which is acceptable in the context of this work. The Ag−C bond length gives the worst agreement, with a difference of approximately 0.3 Å from the experimental value, and is taken into account.

The computed model structure for $Ag_2(dmpm)_2(CN\text{-}tBu)_2^{2+}$ (Figure 4) exhibits an Ag···Ag separation of 2.94 Å, similar to that for **2** (2.9265 Å, X-ray), and a CAgAgC twisted angle of 18°. The first conclusion is that if this structure is correct, as suggested by the $Ag_2(dppm)_2(CN\text{-}tBu)_2^{2+}$ X-ray data, the UV/Vis $d\sigma^* \rightarrow p\sigma$ signature should be present at the same wavelength for both **2** and **6** (see section below). The second point is that the replacement of CN-*t*Bu by dmb should not induce great ring stress or angle torsion.

The computed structure for $Cu_4(dmpm)_6(dmb)_2(CN\text{-}tBu)^{4+}$ exhibits a central bridging dmb ligand adopting a *Z*-conformation (Figure 5). The *U*-form is unfavorable because of important steric hindrance between the $Cu_2$ units. The M···M distance in the M−dmb−M unit is 9.112 Å, which may be slightly overevaluated by 2 × 0.3 Å, as indicated above. The calculated triply bridged Cu···Cu distance is 4.35 Å, predictably longer than that found in **1**, and more similar to the X-ray data for **4** (≈ 4.011 Å). Similarly, the computed NC···CN and N···N distances in the *Z*-dmb are 7.064 and 5.755 Å, respectively. These M···M, C···C, and N···N distances compare favorably to those reported for the crystallographically characterized polymer $\{[Pd_4(dmb)_4(dmb)](MeCO_2)_2\}_n$ (i.e. 9.241, 6.801, and 5.549 Å, respectively).[20]

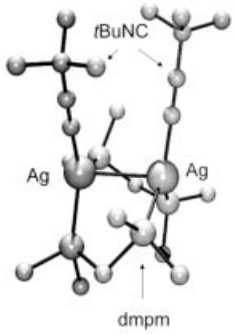


Figure 4. Computed structure for the model compound $Ag_2(dmpm)_2(CN\text{-}tBu)_2^{2+}$; the calculated distances are 2.94, 2.02, 1.20, and 2.47 Å, for the Ag···Ag separation, the AgC, C≡N, and AgP bond lengths, respectively

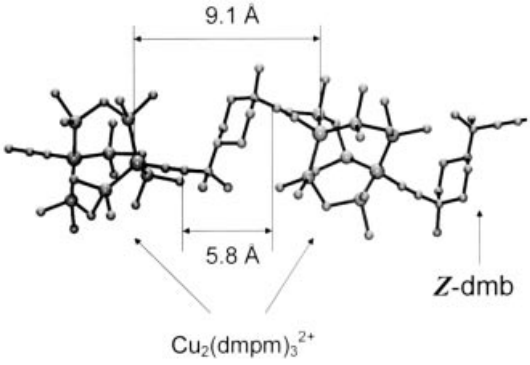


Figure 5. Computed structure for the model compound $Cu_4(dmpm)_6(dmb)_2(CN\text{-}tBu)^{4+}$; the calculated distances are 4.35, 1.83, 1.20, and 2.36 Å, for the Cu···Cu separation, the CuC, C≡N and CuP bond lengths, respectively

### Electronic Spectra

The absorption spectra of compounds **1** and **2** (Figure 6) exhibit an absorption band at about 250 nm. These unstructured bands are due to the $d\sigma^* \rightarrow p\sigma$ transition; an electronic transition that is well-documented for cofacial $d^{10}$-$d^{10}$ species such as $Au_2(dmpm)_3^{2+}$,[38] $Au_2(dcpm)_2^{2+}$ (dcpm = bis(dicyclohexylphosphanyl)-methane),[39] $Au_2(dmpm)_2^{2+}$,[40−42] $M_2(dppm)_3$ (M = Pd, Pt),[43,44] and $Ag_2(dmpm)_2^{2+}$.[45] In order to confirm this assignment, the absorption spectra were also recorded at 77 K in butyronitrile. At this temperature, the bandwidth decreases, in a somewhat similar manner to that of $Pd_2(dppm)_3$[43,44] and $Ag_2(dmpm)_2^{2+}$ [45] (Figure 7). This well-known phenom-

Table 4. Comparison between X-ray data and MMX computations[a]

| | X-ray | | | MMX | | |
|---|---|---|---|---|---|---|
| | *d*(M···M) | *d*(M−P) | *d*(M−C) | *d*(M···M) | *d*(M−P) | *d*(M−C) |
| **1** | 2.9265 | 2.243 | − | 2.978 | 2.267 | − |
| **2** | 2.9893 | 2.434 | − | 2.974 | 2.463 | − |
| $Ag_2(dppm)_2(CN\text{-}tBu)_2^{2+}$ | 3.223 | 2.428 | 2.334 | 3.216 | 2.473 | 2.024 |

[a] All the distances are in Å.

  

enon has been fully described by Gray et al. and others.[46−52] The absorption maxima for the dσ*→pσ bands compare favorably with those of $Au_2(dmpm)_3^{2+}$ rather than with those of other related triply bridged $d^{10}$-$d^{10}$ species (Table 5). No obvious trend is seen along the Cu, Ag, Au series, perhaps reflecting two opposite effects; lengthening of the M···M distance disfavors the M···M interactions, while an increase in atomic radii favors them. The data for **1** agree with that for $[Cu_2(dmpm)_3](ClO_4)_2$ ($\lambda_{max}$ = 264 nm; ε = 7380 $M^{-1}cm^{-1}$ in acetonitrile at 298 K).[26]

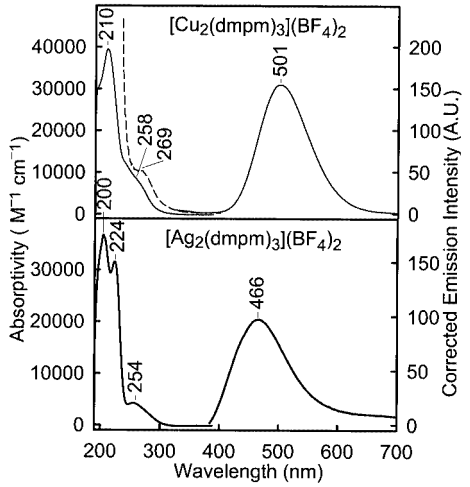


Figure 6. Comparison of the UV/Vis absorption (left) and emission (right) spectra for **1** (top) and **2** (bottom) in acetonitrile at 298 K; the broken line is an example of an excitation spectrum, here for **1**

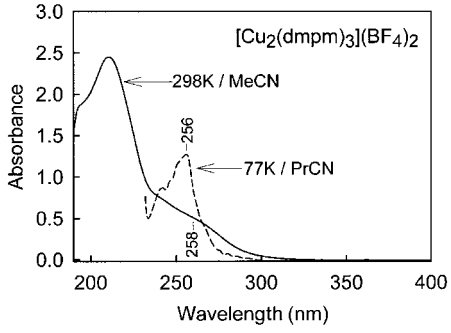


Figure 7. Comparison of the UV/Vis spectra of **1** at 298 K (−) and 77 K (- - -). The lowest wavelength possible is 240 nm at 77 K, because of absorption by the solvent glass

The absorption spectra for **4** and **5** are almost identical to each other, where strong absorptions are observed at 212 and 236, and at 210 and 236 nm, respectively. As anticipated for the noninteracting Cu···Cu systems, the dσ*→pσ absorption is absent. The lowest energy absorption is assigned to the spin-allowed $t_2(d\sigma^*) \rightarrow t_2(\pi^*, p\sigma^*)$ transition.[53,54] Oligomer **6** in acetonitrile exhibits an absorptivity of 10200 $M^{-1}cm^{-1}$ per $Ag_2$ unit for the dσ*→pσ band ($\lambda_{max}$ = 254 nm).

## Emission

The compounds are luminescent in solution at 298 and 77 K (Figures 6 and 8, Table 6), as well as in the solid state. The excitation spectra measured in solution confirm the authenticity of the emission, and the μs timescale for the lifetimes is consistent with a phosphorescence process. Compounds **1** and **2** exhibit luminescence of modest intensity in solution at 298 K at 500 and 471 nm, respectively. The energy gaps between the absorption and emission (18800$cm^{-1}$ for **1**; 17300 $cm^{-1}$ for **2**) are somewhat large. This phenomenon has also been observed for $Au_2(dmpm)_3^{2+}$ by Che, Miskowski et al. ,[38] who have suggested that the emission arises from $^3(d(x^2\text{-}y^2), xy \rightarrow p\sigma)$ excitation, in agreement with Mason's former proposal.[55] The similarity in the absorption maxima and emission lifetimes for **2** and **6** in the solid state strongly suggests that this assignment also applies for oligomer **6**.

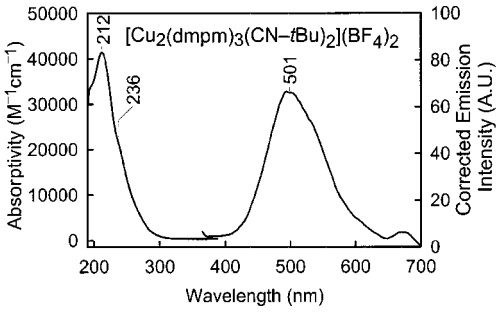


Figure 8. Absorption (left) and emission (right) spectra for **4** in acetonitrile at 298 K

In solution, the emission bands for all compounds are shifted to the red from about 446 nm to 466−520 nm. This range falls in the same region as that for the tetracoordinate Cu species (474−502 nm), and suggests that the emission arising from the tricoordinate Ag species in solution may

Table 5. Comparison of the dσ*→pσ absorption data at 298 K for various $M_2(diphos)_3$ complexes

| | λ (±1 nm) | $\tilde{\nu}$ [$cm^{-1}$] | ε [$M^{-1}cm^{-1}$] | Refs. |
|---|---|---|---|---|
| $[Cu_2(dmpm)_3](BF_4)_2/CH_3CN/298K$ | 258 | 38800 | 8500 | this work |
| $[Ag_2(dmpm)_3](BF_4)_2/CH_3CN/298K$ | 254 | 39400 | 4300 | this work |
| $[Au_2(dmpm)_3](ClO_4)_2/H_2O/298K$ | 256 | 39000 | 18500 | [30] |
| $Pd_2(dppm)_3$/2MeTHF/77K | 440 | 22700 | 33800 | [33] |
| $Pt_2(dppm)_3$/2MeTHF/77K | 488 | 20500 | 27400 | [33] |

  

Table 6. Comparison of the emission spectroscopy and photophysical data (the reported lifetimes are those obtained from the ESM method)

| Compounds | | Solid, 298 K | | Solution,[a] 298 K | | | Solution,[b] 77 K | |
|---|---|---|---|---|---|---|---|---|
| | | $\lambda_{emi}$ [nm] | $\tau_{em}$ [μs] | $\lambda_{emi}$ [nm] | $\tau_e$ [μs][c] | $\Phi_e$ | $\lambda_{emi}$ [nm] | $\tau_e$ [μs] |
| **1** | $[Cu_2(dmpm)_3](BF_4)_2$ | Not measured | | 500 | 16.5 | 0.020 | 505 | 840 |
| **4** | $[Cu_2(dmpm)_3(CN\text{-}t\text{Bu})_2](BF_4)_2$ | 476 | 291 | 501 | 3.8 | 0.0043 | 502 | 712 |
| **5** | $\{[Cu_2(dmpm)_3(dmb)_{1.33}](BF_4)_2\}_3$ | 482 | 257 | 500 | $< 2$ | 0.0013 | 474 | 523 |
| **2** | $[Ag_2(dmpm)_3](BF_4)_2$ | 445 | 41 | 466 | 3.0 | 0.0031 | 482 | 6300 |
| **6** | $\{[Ag_2(dmpm)_2(dmb)_{1.33}](BF_4)_2\}_3$ | 447 | 31 | 520 | $\approx 2$ | 0.0014 | 500 | 542 |

[a] In acetonitrile. [b] In butyronitrile. [c] The detection limit of the instrument is 2 μs, so the accuracy is poor near this limit.

be due to tetracoordinate solvent/anion exciplexes.[39] For the formally tetracoordinate **4** and **5**, the assignment of the emissive state is $^3([t_2(d\sigma^*)]^5[t_2(\pi^*,p\sigma^*)]^1)$ in agreement with that of $M(diphos)_2$ (M = Pd, Pt; diphos = dppe, dppp)[53] and that of $M(CN\text{-}t\text{Bu})_4^+$ (M = Cu, Ag).[15]

The emission lifetime data show two trends (Table 6). First, emission lifetimes predictably increase with the rigidity of the medium, and decrease as the temperature increases. Second, emission lifetimes and quantum yields decrease as the size of the molecule increases. The latter is due to the well-known "loose bolt" effect,[56] where the number of vibrational levels favoring internal conversion increases with the number of groups around the chromophores, as well as with their sizes. It is noteworthy that emission lifetimes for **2** and **6** are significantly longer than those reported for solid $Ag_2(dcpm)_2^{2+}$ at 298 K ($\lambda_{emi}$ = 420 nm; $\tau_e$ = 0.5 μs),[57] and for $Ag_2(dmpm)_2^{2+}$ in ethanol at 77 K ($\lambda_{emi}$ = 371 nm; $\tau_e$ = 49 μs),[45] the latter being dicoordinated.

## Conclusion

The use of an electron-rich phosphane, which renders the metal center more electron-rich, increases the lability of the ligands, in particular that of the isocyanide ligand in this work. This property has a significant effect on the length of the oligomeric materials. This general approach may provide another strategic tool to make the polymer chain shorter for cases where the material would exhibit undesirable properties such as low solubility, preventing easier characterization, and amorphous character in the solid state.

## Experimental Section

**Materials:** 1,8-diisocyano-*p*-menthane[58] was synthesized according to literature procedures. $[Cu(CH_3CN)_4]BF_4$ was freshly prepared before use, following the published procedure.[59] All solvents were purified by standard procedures.[60,61] The following materials were purchased from commercial suppliers: acetone (Fisher), acetonitrile and Cu(m) (Anachemia), petroleum ether and dichloromethane (ACP), ethanol (Les Alcools de Commerce Inc.), dinitrogen and argon (Praxair), $AgBF_4$, $Cu(BF_4)_2{\cdot}xH_2O$ and *tert*-butyl isocyanide (Aldrich Chemicals Co); bis(dimethylphosphanyl)methane (Strem Chemicals Co). Unless otherwise stated, all materials were handled under argon or dinitrogen using standard Schlenk techniques, high-vacuum manifolds and an inert-atmosphere glove box.

**$[Cu_2(dmpm)_3](BF_4)_2$ (1):** $[Cu(CH_3CN)_4]BF_4$ (370.0 mg, 1.18 mmol) was dissolved in acetone (20 mL). The ligand dmpm (0.35 mL, 2.21 mmol) was added dropwise using a microsyringe. The reaction mixture was stirred for 1 h prior to the addition of diethyl ether (80 mL). A white precipitate appeared, which was filtered and dried in a glove box. Yield 60% (315 mg). $^1H$ NMR ($CD_3CN$): δ = 2.02 (m, 6 H, $PCH_2P$), 1.36 (s, 36 H, $PCH_3$) ppm. $^{31}P\{^1H\}$ NMR ($CD_3CN$): δ = −25.36 ppm. $^{13}C\{^1H\}$ NMR ($CD_3CN$): δ = 32.12, 16.12 ppm. UV/Vis ($CH_3CN$): λ (ε) = 210 (39500), 248 nm (8500 $M^{-1}cm^{-1}$). $C_{15}H_{42}B_2Cu_2F_8P_6$ (709.04): calcd. C 25.41, H 5.97; found C 25.45, H 5.90.

**$[Ag_2(dmpm)_3](BF_4)_2$ (2):** $AgBF_4$ (259.6 mg, 1.33 mmol) was dissolved in acetone (15 mL). The resulting solution was filtered prior to use. The ligand dmpm (0.35 mL, 2.21 mmol) was added dropwise with a microsyringe. The solution was stirred for 1 h, and diethyl ether (70 mL) was added to precipitate the white product, which was filtered and dried in vacuo. Yield 90% (478 mg). $^1H$ NMR ($CD_3COCD_3$): δ = 2.45 (m, 6 H, $PCH_2P$), 1.60 (s, 36 H, $PCH_3$) ppm. $^{31}P\{^1H\}$ NMR ($CD_3COCD_3$): δ = −13.98, −15.39, −16.86 ppm. $^{13}C\{^1H\}$ NMR ($CD_3COCD_3$): δ = 31.63, 16.41 ppm. UV/Vis ($CH_3CN$): λ (ε) = 200 (47400), 224 (31400), 254 nm (4300 $M^{-1}cm^{-1}$). $C_{15}H_{42}Ag_2B_2F_8P_6$ (797.68): calcd. C 22.59, H 5.31; found C 22.08, H 5.20.

**$[Ag_2(dmpm)_2](BF_4)_2$ (3):** $AgBF_4$ (53.4 mg, 0.274 mmol) was dissolved in acetone (15 mL). The ligand dmpm (37.5 mg, 0.275 mmol) was added dropwise using a microsyringe. The solution was stirred for 1 h, prior to adding diethyl ether (70 mL). The white precipitate was filtered and dried under an inert atmosphere. Yield 76% (90.6 mg). $^1H$ NMR ($CD_2Cl_2$): δ = 2.31 (m, 4 H, $PCH_2P$), 1.61 (s, 24 H, $PCH_3$) ppm. $^{31}P\{^1H\}$ NMR ($CD_2Cl_2$): δ = −12.99 (br d, $J$(AgP) = 560 Hz) ppm. $^{13}C\{^1H\}$ NMR ($CD_3CN$): δ = 30.01, 14.46 ppm. UV/Vis ($CH_3CN$): λ (ε) = 202 (48000), 256 nm (23400 $M^{-1}cm^{-1}$). $C_{10}H_{28}Ag_2B_2F_8P_4$ (661.57): calcd. C 18.15, H 4.27; found C 18.24, H 4.32.

**$[Cu_2(dmpm)_3(CN\text{-}t\text{Bu})_2](BF_4)_2$ (4):** Compound **1** (102.1 mg, 0.144 mmol) was dissolved in degassed acetone (30 mL). *t*BuNC (0.1 mL, 0.88 mmol) was added dropwise using a microsyringe. The solution was stirred for 1 h prior to being concentrated in vacuo to a volume of 5 mL. Dimethyl ether (25 mL) was added to precipitate a white solid, which was filtered and dried in vacuo. Yield 86% (108 mg). $^1H$ NMR ($CD_3COCD_3$): δ = 2.26 (m, 6 H, $PCH_2P$): 1.59 [s, 18 H, $(CH_3)_3C$], 1.45 (s, 36 H, $PCH_3$) ppm. $^{31}P\{^1H\}$ NMR ($CD_3COCD_3$): δ = −25.41ppm. $^{13}C\{^1H\}$ NMR ($CD_3COCD_3$): δ = 58.38, 33.03, 30.20, 17.84 ppm. IR (KBr): 1052 ($\nu_{BF}$), 2177

  

($\nu_{C\equiv N}$) $cm^{-1}$. Raman (solid): 2176 ($\nu_{C\equiv N}$) $cm^{-1}$. UV/Vis ($CH_3CN$): λ (ε) = 212 (39500), 236 (sh.) nm (22200 $M^{-1}cm^{-1}$). $C_{25}H_{60}B_2Cu_2F_8N_2P_6$ (875.30): calcd. C 34.30, H 6.91, N 3.20; found C 34.03, H 6.74, N 3.02.

**{[$Cu_2$(dmpm)$_3$(dmb)$_{1.33}$][$(BF_4)_2$}$_3$ (5):** Compound **1** (106.2 mg, 0.150 mmol) was dissolved in degassed acetone (20 mL). The ligand dmb (100.0 mg, 0.525 mmol) was dissolved separately in a round-bottom flask containing degassed acetone (150 mL). This solution was added dropwise and slowly to the former solution, and the mixture was stirred for 4 h prior to being concentrated in vacuo to a volume of 15 mL. Diethyl ether (150 mL) was added. A white product precipitated, which was filtered and dried. Yield 52% (86.9 mg). $^1H$ NMR ($CD_3CN$): δ = 2.08−2.02 (m, 8 H, dmb), 2.01 (m, 18 H, $PCH_2P$), 1.87−1.83 (m, 8 H, dmb), 1.61−1.56 (m, 12 H, dmb), 1.51 (s, 20 H, dmb), 1.45 (s, 24 H, dmb), 1.35 (s, 108 H, $CH_3P$) ppm. $^{31}P\{^1H\}$ NMR ($CD_3CN$): δ = −25.55 ppm. $^{13}C\{^1H\}$ NMR ($CD_3CN$): δ = 60.45, 63.18, 45.32, 37.10, 32.55, 29.11, 26.05, 23.32, 7.18 ppm. IR (KBr): $\tilde{\nu}$ = 1052 ($\nu_{BF}$), 2161 ($\nu_{C\equiv N}$) $cm^{-1}$. Raman (solid): 2160 ($\nu_{C\equiv N}$) $cm^{-1}$. UV/Vis ($CH_3CN$): λ (ε) = 210 (51100), 236 (sh.) nm (26500 $M^{-1}cm^{-1}$). $C_{93}H_{198}B_6Cu_6F_{24}N_8P_{18}$ (2888.25): calcd. C 38.67, H 6.91, N 3.88; found C 38.64, H 6.79, N 4.02.

**{[$Ag_2$(dmpm)$_2$(dmb)$_{1.33}$][$(BF_4)_2$}$_3$ (6):** Compound **3** (59.1 mg, 0.089 mmol) was dissolved in degassed acetone (45 mL). The ligand dmb (53 mg, 0.279 mmol) was dissolved separately in a round-bottom flask containing degassed acetone (60 mL). This solution was added dropwise and slowly to the former solution, and the mixture was stirred for 3 h prior to being concentrated in vacuo to a volume of 15 mL. Diethyl ether (120 mL) was added to precipitate the white product, which was filtered and dried in vacuo. Yield 99% (76.1 mg). $^1H$ NMR ($CD_2Cl_2$): δ = 2.16 (m, 12 H, $PCH_2P$), 2.03−1.85 (m, 16 H, dmb) 1.53 (s, 88 H, $CH_3P$ + dmb) 1.50−1.43 (m, 40 H, dmb) ppm. $^{31}P\{^1H\}$ NMR ($CD_2Cl_2$): δ = −15.68 (m) ppm. $^{13}C\{^1H\}$ NMR ($CD_3COCD_3$): δ = 64.12, 61.21, 43.78, 36.92, 31.96, 28.25, 27.21, 22.88, 16.44, 15.56 ppm. IR (KBr): $\tilde{\nu}$ = 1051 ($\nu_{BF}$), 2181 ($\nu_{C\equiv N}$) $cm^{-1}$. Raman (solid): 2182 ($\nu_{C\equiv N}$) $cm^{-1}$. UV/Vis ($CH_3CN$): λ (ε) = 198 (40300), 254 nm (10200 $M^{-1}cm^{-1}$). $C_{78}H_{156}Ag_6B_6F_{24}N_8P_{12}$ (2745.85): calcd. C 34.12, H 5.73, N 4.08; found C34.29, H 5.32, N 3.96.

**Apparatus:** All NMR spectra were acquired using a Bruker AC-300 spectrometer ($^1H$ 300.15 MHz, $^{13}C$ 75.48 MHz, $^{31}P$ 121.50 MHz) using the solvent as the chemical shift standard, except for $^{31}P$ NMR, where the chemical shifts are relative to external $D_3PO_4$ 85% in $D_2O$. IR spectra were acquired on a Bomem FT-IR MB series spectrometer equipped with a baseline-diffused reflectance. UV/Vis spectra were acquired using a Hewlett Packard diode array 8452A spectrophotometer . Continuous wave emission and excitation spectra were obtained using a SPEX Fluorolog II spectrometer. Emission lifetimes were measured with a nanosecond $N_2$ laser system (PTI) model GL-3300 pumping a dye laser model GL-302. The excitation wavelength was 311 nm for all the measurements. MALDI-TOF mass spectra were acquired on a Bruker Proflex III linear mode spectrometer with a nitrogen laser (337 nm) at the Université de Bourgogne in Dijon (France) using a dithranol matrix. Glass transition temperatures ($T_g$) were measured with a Perkin−Elmer 5A DSC7 equipped with a thermal controller 5B TAC 7/DS. Calibration standards were water and indium. FT-Raman spectra were acquired on a Bruker RFS 100/S spectrometer. XRD were acquired on a Rigaku/USA Inc with a copper lamp operating under a 30 mA current and a 40 kV tension. TGA were acquired on a TGA 7 of Perkin−Elmer between 50 and 650 °C at 3°C/minute under $N_2$.

**Crystallography:** Crystals of [$Ag_2$(dmpm)$_3$][$(BF_4)_2$ (**2**) were grown by vapor diffusion using acetonitrile/*tert*-butylmethyl ether at 23 °C, crystals of [$Cu_2$(dmpm)$_3$][$(BF_4)_2$ (**1**) were grown by vapor diffusion using acetone/*tert*-butylmethyl ether at 23 °C (data see Table 7). Single crystals were coated with Paratone-N oil, mounted on a glass fiber and frozen in the cold nitrogen stream of the goniometer. A hemisphere of data was collected on a Bruker AXS P4/SMART 1000 diffractometer using ω and θ scans with a scan width of 0.3° and 10 s exposure times. The detector distance was 5 cm. The data were reduced (SAINT)[62] and corrected for absorption (SADABS).[63,64] The structure was solved by direct methods and refined by full-matrix least-squares on F[63,64] (SHELXTL).[63,64] All non-hydrogen atoms were refined anisotropically. Hydrogen atoms were found in Fourier difference maps and refined isotropically. Thermal ellipsoid plots are at the 30% probability level. In some plots, hydrogen atoms have been omitted for clarity.

Table 7. Crystal data for **1** and **2**

| | [$Cu_2$(dmpm)$_3$][$(BF_4)_2$ | [$Ag_2$(dmpm)$_3$][$(BF_4)_2$ |
|---|---|---|
| Empirical formula | $C_{15}H_{42}B_2Cu_2F_8P_6$ | $C_{15}H_{42}Ag_2B_2F_8P_6$ |
| Molecular mass | 709.01 | 797.67 |
| Temperature [K] | 198(1) | 198(1) |
| Wavelength [Å] | 0.71073 | 0.71073 |
| Crystal system | monoclinic | orthorhombic |
| Space group | $P2_1/c$ | *Pbca* |
| *a* [Å] | 16.9960(9) | 13.9467(7) |
| *b* [Å] | 11.0485(5) | 14.6460(8) |
| *c* [Å] | 16.9515(9) | 31.6720(17) |
| β [°] | 99.258(1) | 90 |
| Volume [$Å^3$] | 3141.7(3) | 6469.4(6) |
| *Z* | 4 | 8 |
| *d* (calcd) [$Mg/m^3$] | 1.499 | 1.638 |
| Reflections collected | 22019 | 43787 |
| Independent reflections | 7131 | 7391 |
| Goodness-of-fit | 1.085 | 1.037 |
| *R*1[a] | 0.0299 | 0.0202 |
| *wR*2[a] | 0.0824 | 0.0499 |

[a] $R1 = \||F_o| - |F_c|\| / |F_o|$; $wR2 = \{[w(F_o^2-F_c^2)^2]/[F_o^4]\}^{1/2}$; (**1**): weight = $1/[\sigma^2(F_o^2) + (0.0528P)^2 + (0.9190P)]$ and (**2**): weight = $1/[\sigma^2(F_o^2) + (0.0463P)^2 + (1.7267P)]$, where $P = [\max(F_o^2, 0) + 2F_c^2]/3$.

**Procedures:** The emission quantum yields were measured using 9,10-diphenylanthracene as the standard ($\Phi_F$ = 1.00 for degassed solutions).[65] The emission lifetimes were analyzed in two ways. The first way was the common deconvolution method allowing for analysis of the raw data using models with 1−4 exponential decays. The second way was the ESM (Exponential Series Method),[66,67] which gave a distribution of lifetimes instead of a single value, and the maximum of the distribution was retained. Both methods gave the same results, but ESM gave better fits. The quality of the fit between the experimental and calculated curves was addressed using the parameter χ (goodness of fit), and by the analysis of the residual.

**Computer Modeling:** The calculations were performed using the commercially available PC-Model from Serena Software (version 7.0), which uses the MMX empirical model. Comparisons between literature X-ray structures and computed models are provided in the text. The R−N≡C groups are replaced by R−C≡$C^-$ because PC Model does not model C≡$N^+$− fragments, as strongly bent

  

structures had to be calculated. Instead −C≡C− is used securing a more linear and realistic frame for the ligand.

CCDC-245030 (for **2**) and -245031 (for **1**) contain the supplementary crystallographic data for this paper. These data can be obtained free of charge at www.ccdc.cam.ac.uk/conts/retrieving.html [or from the Cambridge Crystallographic Data Centre, 12 Union Road, Cambridge CB2 1EZ, UK; Fax: (internat.) +44-1223-336-033; E-mail: deposit@ccdc.cam.ac.uk].

## Acknowledgments

This research was supported by the Natural Sciences ad Engineering Research Council of Canada (NSERC). P.D.H. thanks Dalila Samar for technical assistance.

[1] S. L. James, *Chem. Soc. Rev.* **2003**, *32*, 276−288.
[2] E. Lozano, M. Nieuwenhuyzen, S. L. James, *Chem. Eur. J.* **2001**, *7*, 2644−2651.
[3] F. Mohr, M. C. Jennings, R. J. Puddephatt, *Angew. Chem. Int. Ed.* **2004**, *43*, 969−971.
[4] R. J. Puddephatt, *Coord. Chem. Rev.* **2001**, *216−217*, 313−332.
[5] P.-S. Kim, M.-C. Brandys, Y. Hu, R. J. Puddephatt, T.-K. Sham, *J. Luminescence* **2003**, *105*, 21−26.
[6] T. J. Burchell, D. J. Eisler, M. C. Jennings, R. J. Puddephatt, *Chem. Commun.* **2003**, 2228−2229.
[7] R. J. Puddephatt, *Macromol. Symp.* **2003**, *196*, 137−144.
[8] W. J. Hunks, M. C. Jennings, R. J. Puddephatt, *Chem. Commun.* **2002**, 1834−1835.
[9] M.-C. Brandys, R. J. Puddephatt, *J. Am. Chem. Soc.* **2002**, *124*, 3946−3950.
[10] A. Adolf, M. Gonsior, I. Krossing, *J. Am. Chem. Soc.* **2002**, *124*, 7111−7116.
[11] S.-M. Kuang, Z.-Z. Zhang, Q.-G. Wang, T. C. W. Mak, *Chem. Commun.* **1998**, 581−582.
[12] I. Ino, J. C. Zhong, M. Manukata, T. Kudora-Sowa, M. Maekawa, M. Suenaga, Y. Kitamori, *Inorg. Chem.* **2000**, *39*, 4273−4279.
[13] P. D. Harvey, *Polymer Preprint* **2004**, *45*, 433−434.
[14] P. D. Harvey, *Macromol. Symp.* **2004**, *209*, 81−95.
[15] D. Fortin, M. Drouin, M. Turcotte, P. D. Harvey, *J. Am. Chem. Soc.* **1997**, *119*, 531−541.
[16] D. Perreault, M. Drouin, A. Michel, P. D. Harvey, *Inorg. Chem.* **1992**, *31*, 3688−3689.
[17] É. Fournier, F. Lebrun, A. Decken, P. D. Harvey, *Inorg. Chem.* **2004**, *43*, 3127−3135.
[18] M. Turcotte, P. D. Harvey, *Inorg. Chem.* **2002**, *41*, 2971−2974.
[19] D. Fortin, M. Drouin, P. D. Harvey, *J. Am. Chem. Soc.* **1998**, *120*, 5351−5352.
[20] T. Zhang, M. Drouin, P. D. Harvey, *Inorg. Chem.* **1999**, *38*, 1305−1315.
[21] T. Zhang, M. Drouin, P. D. Harvey, *Inorg. Chem.* **1999**, *38*, 957−963.
[22] É. Fournier, S. Sicard, A. Decken, P. D. Harvey, *Inorg. Chem.* **2004**, *43*, 1491−1501.
[23] S. Sicard, J.-F. Bérubé, D. Samar, A. Massaoudi, F. Lebrun, J.-F. Fortin, D. Fortin, A. Decken, P. D. Harvey, *Inorg. Chem.* **2004**, *43*, in press.
[24] P. A. Dean, J. J. Vittal, R. S. Srivastava, *Can. J. Chem.* **1987**, *65*, 2628−2633.
[25] D. Perreault, M. Drouin, A. Michel, V. M. Miskowski, W. P. Schaefer, P. D. Harvey, *Inorg. Chem.* **1992**, *31*, 695−702.
[26] Z. Mao, H.-Y. Chao, Z. Hui, C.-M. Che, W.-F. Fu, K.-K. Cheung, N. Zhu, *Chem. Eur. J.* **2003**, *9*, 2885−2894.
[27] P. D. Harvey, *Coord. Chem. Rev.* **2001**, *219−221*, 17−52.
[28] D. Fortin, M. Drouin, P. D. Harvey, F. G. Herring, D. A. Summers, R. C. Thompson, *Inorg. Chem.* **1999**, *38*, 1253−1260.
[29] D. Perreault, M. Drouin, A. Michel, P. D. Harvey, *Inorg. Chem.* **1993**, *32*, 1903−1912.
[30] W. Bensch, M. Prelati, W. Ludwig, *J. Chem. Soc., Chem. Commun.* **1986**, 1762−1763.
[31] F. A. Cotton, G. Wilkinson, P. Gaus, *Basic Inorganic Chemistry*, Wiley, New York, **1995**, p.61.
[32] U.M. Tripathi, A. Bauer, H. Schmidbaur, *J. Chem. Soc., Dalton Trans.* **1997**, 2865.
[33] R. V. Kirss, R. Eisenberg, *Inorg. Chem.* **1989**, *28*, 3372−3380.
[34] L. J. Manojlovic-Muir, K. W. Muir, M. C. Grossel, M. P. Brown, C. D. Nelson, A. Yavari, E. Kallas, R. P. Moulding, K. R. Seddon, *J. Chem. Soc., Dalton Trans.* **1986**, 1955−1963.
[35] H. H. Karsch, U. Schubert, *Z. Naturforsch., Teil B* **1982**, *37*, 186−189.
[36] P. D. Harvey, M. Drouin, T. Zhang, *Inorg. Chem.* **1997**, *36*, 4998−5005.
[37] S. S. M. Ling, I. R. Jobe, A. J. McLennan, L. J. Manojlovic-Muir, K. W. Muir, R. J. Puddephatt, *J. Chem. Soc., Chem. Commun.* **1985**, 566−567.
[38] K. H. Leung, D. L. Phillips, Z. Mao, C.-M. Che, V. M. Miskowski, C.-M. Chan, *Inorg. Chem.* **2002**, *41*, 2054−2059.
[39] H.-X. Zhang, C.-M. Che, *Chem. Eur. J.* **2001**, *7*, 4887−4893.
[40] W.-F. Fu, K.-C. Chan, K.-K. Cheung, C.-M. Che, *Chem. Eur. J.* **2001**, *7*, 4656−4664.
[41] K. H. Leung, D. L. Phillips, M.-C. Tse, C.-M. Che, V. M. Miskowski, *J. Am. Chem. Soc.* **1999**, *121*, 4799−4803.
[42] W.-F. Fu, K.-C. Chan, V. M. Miskowski, C.-M. Che, *Angew. Chem. Int. Ed.* **1999**, *38*, 2783−2785.
[43] P. D. Harvey, H. B. Gray, *J. Am. Chem. Soc.* **1988**, *110*, 2145−2147.
[44] P. D. Harvey, R. F. Dallinger, W. H. Woodruff, H. B. Gray, *Inorg. Chem.* **1989**, *28*, 3057−3059.
[45] D. Piché, P. D. Harvey, *Can. J. Chem.* **1994**, *72*, 705−713.
[46] V. M. Miskowski, T. P. Smith, T. M. Loehr, H. B. Gray, *J. Am. Chem. Soc.* **1985**, *107*, 7925−7934.
[47] R. A. Levenson, H. B. Gray, *J. Am. Chem. Soc.* **1975**, *97*, 6042−6047.
[48] M. S. Wrighton, D. S. Ginley, *J. Am. Chem. Soc.* **1975**, *97*, 4246−4251.
[49] H. B. Abrahamson, C. C. Frazier, D. S. Ginley, H. B. Gray, J. Lilienthal, D. R. Tyler, M. S. Wrighton, *Inorg. Chem.* **1977**, *16*, 1554−1556.
[50] D. R. Tyler, R. A. Levenson, H. B. Gray, *J. Am. Chem. Soc.* **1978**, *100*, 7888−7893.
[51] J. Markham, *J. Rev. Mod. Phys.* **1959**, *31*, 956−989.
[52] P. D. Harvey, Z. Murtaza, *Inorg. Chem.* **1993**, *32*, 4721−4729.
[53] P. D. Harvey, W. P. Schaefer, H. B. Gray, *Inorg. Chem.* **1988**, *27*, 1101−1104.
[54] A. A. Orio, B. B. Chastain, H. B. Gray, *Inorg. Chim. Acta* **1969**, *3*, 8−10.
[55] M. M. Savas, W. R. Mason, *Inorg. Chem.* **1987**, *26*, 301−307.
[56] N. J. Turro, *Modern Molecular Photochemistry*, Benjamen/Cummings Pub. Co., Menlo Park, **1978**, p. 235.
[57] C.-M. Che, M.-C. Tse, M. C. W. Chan, K.-K. Cheung, D. L. Phillips, K. H. Leung, *J. Am. Chem. Soc.* **2000**, *122*, 2464−2468.
[58] W. D. Weber, G. W. Gokel, I. K. Ugi, *Angew. Chem. Int. Ed. Engl.* **1972**, *11*, 530−531.
[59] B. J. Hathaway, D. G. Holah, J. D. Postlethwaite, *J. Chem. Soc.* **1961**, 3215−3218.
[60] D. D. Perrin, W. L. F. Armarego, D. R. Perrin, *Purifications of Laboratory Chemicals*, Pergamon, Oxford, **1966**.
[61] A. J. Gordon, R. A. Ford, *The Chemist's Companion, a Handbook of Practical Data, Techniques, and References*, Wiley, New York, **1972**, p. 436.
[62] *SAINT 6.02*, Bruker AXS, Inc., Madison, Wisconsin, **1997−1999**.
[63] *SADABS*, George Sheldrick, Bruker AXS, Inc., Madison, Wisconsin, **1999**.

  

[64] *SHELXTL 5.1*, George Sheldrick, Bruker AXS, Inc., Madison, Wisconsin, **1997**.
[65] E. C. Lim, J. D. Laposa, J. M. H. Yu, *J. Mol. Spectrosc.* **1966**, *19*, 412−420.
[66] A. Siemiarczuk, B. D. Wagner, W. R. Ware, *J. Phys. Chem.* **1990**, *94*, 1661−1666.
[67] A. Siemiarczuk, W. R. Ware, *Chem. Phys. Lett.* **1989**, *160*, 285−290.

Received June 20, 2004
Early View Article
Published Online September 9, 2004

  